Optimal Immunotherapy Interactions in Oncolytic Viral Therapy and Adopted Cell Transfer for Cancer Treatment with Saturation Effects

G. V. R. K. VITHANAGE[1], SOPHIA R-J JANG[2]
[1]Department of Mathematical Sciences,
Wayamba University of Sri Lanka, Kuliyapitiya,
SRI LANKA

[2]Department of Mathematics and Statistics,
Texas Tech University,
Lubbock, TX, 79409,
USA

Abstract: - Scientists worldwide employ various cancer treatment methods, including Oncolytic Viral Therapy (OVT) and Adoptive Cell Transfer (ACT). In this study, we investigate the efficacy of combined therapies over short durations using optimal control theory strategies. We establish the existence of an optimal control pair and derive the necessary conditions. Using MATLAB, we conduct computational analyses and plot time series of susceptible tumour populations with and without therapy, as well as the behaviour of the control pair over time. This analysis identifies key parameters and dosages for effective cancer control. Our research aims to minimize the number of susceptible tumour cells and reduce therapy-related costs over the treatment period. We observe that combined therapy yields limited therapeutic outcomes compared to OVT and ACT alone. However, increasing the tumour-killing rate by immune cells enhances the effectiveness of both OVT and ACT therapies. This innovation holds promise for eliminating tumour cells using genetically modified viruses and immune cells.

Key-Words: - Michaelis-Menten, Optimal Control, Susceptible Tumor, Runge-Kutta Scheme, Oncolytic Viral Therapy, Adoptive Cell Transfer.

Received: May 16, 2024. Revised: December 18, 2024. Accepted: January 14, 2025. Published: March 28, 2025.

1 Introduction

Cancer is a complex disease responsible for many deaths worldwide. According to the World Health Organization nearly 10 million deaths occurred in 2020 alone. It is characterized by the uncontrolled growth of abnormal cells that defy the normal rules of cell division. Throughout history, various therapies have been employed to treat cancer, but these methods have often proven insufficient in addressing persistent cancers. Consequently, there is a need for alternative treatment approaches to eradicate tumour cells.

Today, cancer immunotherapy has emerged as a leading strategy for treating cancer through various approaches, [1]. This treatment method involves activating immune system's ability to combat cancer, [1], [2], [3]. In cancer immunotherapy, the individual's own immune system is utilized to target cancer cells. This approach can augment or modify the immune system's function, enabling it to effectively attack cancer cells. Adoptive cell transfer is a successful method within cancer immunotherapy, where T cells are used to fight cancer. T cells, a type of immune cell, are potent weapons of the immune system, targeting cancer cells. These T cells are extracted from the patient's body, enhanced in a laboratory to produce millions of copies, and then reintroduced into the patient. Oncolytic viral therapy has gained prominence as a modern cancer treatment method. This approach uses viruses to target cancer cells, with some viruses engineered specifically to combat cancer, known as oncolytic viruses (OVs). These OVs are either genetically modified or naturally occurring viruses that selectively replicate in and destroy cancer cells while sparing normal tissues, [3], [4].

Constructing mathematical models for the tumor and immune system interactions is challenging. These models serve as powerful tools for studying and describing the dynamic behavior of tumor-immune interactions, [5]. In our model, we consider susceptible tumor populations, infected tumor populations, viral populations, and immune cell

populations. Both immune cells and oncolytic viral cells target tumor cells, and the interaction between tumor cells and immune cells can be studied using works such as [6], [7]. A recent study, proposed a mathematical model in [8], which considers the proliferation and exhaustion of immune cells through a single parameter.

More recently [9] proposed and investigated a mathematical model of tumor-immune system interactions with oncolytic viral therapy. This model incorporates both immune exhaustion and proliferation with saturation effects. Using this result we have revealed that immunosuppression can enhance the effectiveness of OVT, while a weak immune response may increase the risk of tumor recurrence.

Here, we apply optimal control techniques to the model introduced in [9]. Our primary objective is to investigate the short-term treatment effects of Adoptive Cell Transfer (ACT) and Oncolytic Viral Therapy (OVT), with the goal of minimizing both tumour size and therapy costs. While previous studies have explored the optimal control effects on OVT individually, none have examined the combined therapy, [10], [11]. Optimal Control Theory, a branch of mathematics, allows us to optimize the solution of the system. By employing the Classical Theory of Optimal Control [12], we first establish the existence of an optimal control pair. Although the model has only one positive equilibrium, it includes three boundary equilibria. Our goal is to design an optimal immunotherapy regimen using techniques from optimal control theory.

First, we introduce the optimal control problem. Then, in Section 3, we apply Pontryagin's Maximum Principle to derive the necessary conditions and the optimality system. Pontryagin's Maximum Principle is a set of conditions that must be satisfied for an optimization problem to be solved optimally. In Section 4, we provide numerical examples illustrating monotherapy with OVT, ACT, and combined OVT and ACT. We conclude in Section 5.

2 The Mathematical Model

We begin by outlining the model we are using for optimal control techniques. This model consists of four state variables: x representing the susceptible tumor population, y representing the infected tumor population, v denoting the compartment of free viral particles, and z representing immune cells. The units for cell populations are given in cell numbers, while the unit for viral particles is in pfu (plaque-forming units), with time measured in days. Experimental results clearly indicate that logistic growth is appropriate for larger tumor sizes both in vivo and in vitro. We employ the logistic growth model to describe the growth of the susceptible tumor population, characterized by an intrinsic growth rate r and a carrying capacity of $1/b$ for all tumor cells, [12], [13], [14], [15].

The infection of viral cells is modeled using the famous Michaelis Menten term with a half-saturation constant g and a high infection rate β. The rate at which susceptible tumor cells are killed by immune cells is denoted by k, while the corresponding killing rate of infected tumour cells by immune cells is given by c. Infected tumour cells face to additional death rate a due to infection. The viral burst size per infected tumour cell is denoted by q. The killing rate of OVT cells by immune cells is modelled using the mass action law with γ. The natural death rates of viruses and immune cells are constant and denoted by δ and d, respectively. It is assumed that there is a constant supply of immune cells from the lymph nodes into the tumour microenvironment at a rate s. As in our previous model, we also use a Michaelis-Menten mechanism to model the activation from infected tumour cells, with p denoting the maximum rate and h the half-saturation constant.

$$\begin{aligned} x' &= rx\big(1 - b(x+y)\big) - \frac{\beta x v}{g+x} - kxz \\ y' &= \frac{\beta x v}{g+x} - ay - cyz \\ v' &= qay - \delta v - \gamma vz \\ z' &= s - dz + \frac{b_e xz}{k_e + x} - \frac{d_e xz}{k_d + x} + \frac{pyz}{h+y} \end{aligned} \tag{1}$$

$$x(0) > 0, y(0) \geq 0, x(0) + y(0) < \tfrac{1}{b},$$
$$v(0) \geq 0, z(0) \geq 0$$

All parameters in this model are positive. To account for saturation effects in the proliferation of immune cells, we introduce be as the maximum proliferation rate and de as the maximum exhaustion rate of immune cells. The corresponding half-saturation constants are denoted by k_e and k_d, respectively. This model is a modified version of our previous research on optimal control in tumor virus system interactions, [16]. The study in, provides sufficient conditions, based on the model parameters, under which the tumor can eliminate for all sizes. However, achieving complete tumor elimination may take a long period, potentially exceeding the patient's lifetime.

3 Optimal Control Problem

In this section, we aim to apply optimal control techniques. As discussed in the previous section, the results derived in [16], focus on the long-term dynamics of tumor behavior. Here, first we use optimal control strategies to explore the short-term effects of viral therapy and immunotherapy on tumor regression.

The goal is to minimize both tumor size and the costs associated with implementing immunotherapies over the treatment period$[0,T]$, where $T>0$ is fixed. Let $s_1 \geq 0$ and $s_2 \geq 0$ represent the strengths of oncolytic viral therapy (OVT) and adoptive cell transfer (ACT) according to $s_1 + s_2 > 0$. The controls for OVT and ACT are denoted by $u_1(t)$ and respectively. Specifically, the units of s_1 and s_2 are $pfu\ day^{-1}$ and $cell\ day^{-1}$, respectively, while $u_1(t)$ and $u_2(t)$, are dimensionless. The state equations are expressed as follows.

$$\begin{aligned} x' &= rx\big(1-b(x+y)\big) - \frac{\beta x v}{g+x} - kxz \\ y' &= \frac{\beta x v}{g+x} - ay - cyz \\ v' &= qay - \delta v - \gamma vz + s_1 u_1(\mathrm{t}) \\ z' &= s - dz + \frac{b_e xz}{k_e + x} - \frac{d_e xz}{k_d + x} + \frac{pyz}{h+y} s_2 u_2(\mathrm{t}) \end{aligned} \tag{2}$$

$$x(0) > 0, y(0) \geq 0, x(0) + y(0) < \tfrac{1}{b},$$
$$v(0) \geq 0, z(0) \geq 0$$

Since the goal is to minimize the susceptible tumour size and the costs of implementing immunotherapies over the treatment period$[0,T]$, the objective functional is given by:

$$J(u_1,u_2) = \int_0^T \big(x(t) + \tfrac{c_1}{2}\big(u_1(t)\big)^2 + \tfrac{c_2}{2}\big(u_2(t)\big)^2\big)dt \tag{3}$$

Where (u_1,u_2) belong to the class

$$U = \{(u_1,u_2): u_i(t) \text{ is piecewise continuous with } 0 \leq u_i(t) \leq 1 \text{ on } [0,T], i = 1,2\} \tag{4}$$

The parameters $c_1 \geq 0$ and $c_2 \geq 0$ are the weighted constants used to balance the contributions between the two types of treatment. We assume $c_i > 0$ if $s_i > 0$. The optimal control problem consists of

$$\min_{(u_1,u_2) \in U} J(u_1,u_2) \tag{5}$$

subject to the state equations (1).

Establishing the existence of optimal controls is a basic step in optimization. After outlining the optimal control problem, we will explore the existence of optimal controls, their characterizations, and the optimality system in the subsequent subsections.

3.1 Existence of Optimal Control Pair

The classical theory of optimal control, [17], can be applied directly to analyze the problem formulated in (3.1)–(3.4). We will begin by verifying the existence of an optimal control

Theorem 3.1. There exists an optimal control pair for the problem 3.1-3.4.

Proof. It is enough to show that the following conditions given in Corollary 4.1 of [17], are satisfied.

(a) The set of all initial conditions with a control pair $(u_1,u_2) \in U$ for which the state equations being satisfied is nonempty.

(b)U is closed and convex.

(c) The right-hand side of each of the state equations is continuous, bounded above by the sum of the control and the state, and can be written as a linear function of $u_1(t)$, $u_2(t)$, with coefficients depending on time.

(d)The integrand of $J(u_1,u_2)$ is convex in U and is bounded below by $-k_2 + k_1|(u_1,u_2)|^\eta$ with $k_1 > 0\ and\ \eta > 1$.

Clearly for each fixed initial condition and control pair (1) has a unique solution on $[0,T]$ and (a) is satisfied. Moreover, as $x'|_{x=0} = 0, y'|_{x=0} \geq 0$ and $v'|_{v=0} \geq 0, z'|_{z=0} \geq 0$, solutions remain non negative on $[0,T]$. It is obvious that (b) is true and (d) is satisfied with $\eta = 2$. To verify (c), notice $x(t) > 0, y(t) \geq 0, v(t) \geq 0, z(t) \geq 0$ and $x(t) + y(t) < \frac{1}{b}$
for all $t \in [0,T]$. Thus $x' \leq rx$, $y' \leq \beta v - ay, v' \leq qay - \delta v + s_1 u_1(t)$ and $z' \leq s - dz + pz + \frac{b_e z}{b} + s_1 u_1(t)$

$$\begin{pmatrix} x' \\ y' \\ v' \\ z' \end{pmatrix} \leq M \begin{pmatrix} x \\ y \\ v \\ z \end{pmatrix} + \begin{pmatrix} 0 \\ 0 \\ s_1 u_1(t) \\ s + s_2 u_2(t) \end{pmatrix}$$

where

$$M = \begin{pmatrix} r & 0 & 0 & 0 \\ 0 & -\alpha & \beta & 0 \\ 0 & qa & -\delta & 0 \\ 0 & 0 & 0 & -d + \frac{b_e}{b} + p \end{pmatrix}$$

Let $x = (x, y, v, z)^{tr}$, the transpose of (x, y, v, z). Then

$$||\frac{dX}{dt}|| = ||M||.||\begin{pmatrix} x \\ y \\ v \\ z \end{pmatrix}|| + ||\begin{pmatrix} 0 \\ 0 \\ s_1 u_1(t) \\ s + s_2 u_2(t) \end{pmatrix}||$$

Thus (c) is verified and there exists an optimal control pair for the control problem (2)–(3) by [17].

3.2 The Adjoint System and Control Pair

We next apply the Pontryagin's Maximum Principle to derive necessary conditions, [18]. Let $\lambda_1, \lambda_2, \lambda_3, \lambda_4$ denote the adjoint vector. The Hamiltonian of the optimal control problem (1)-(5) is:

$$\begin{aligned} &H(x, y, v, z, \lambda_1, \lambda_2, \lambda_3, \lambda_4) = x + \frac{c_1}{2}u_1^2 + \frac{c_2}{2}u_2^2 \\ &+\lambda_1(rx\big(1 - b(x + y)\big) - \frac{\beta xv}{x+g} - kxz) \\ &+\lambda_2(\frac{\beta xv}{x+g} ay)cyz \\ &+\lambda_3(qay - \delta v - \gamma vz + s_1 u_1) \\ &+\lambda_4(s - dz + \frac{b_e xz}{k_e + x} - \frac{d_e xz}{k_d + x} + \frac{pyz}{h+y}) \end{aligned} \quad (6)$$

Where the adjoint variables satisfy $\lambda_1' = -\frac{\partial H}{\partial x}, \lambda_2' = -\frac{\partial H}{\partial y}, \lambda_3' = -\frac{\partial H}{\partial v}, \lambda_4' = -\frac{\partial H}{\partial z}$ with the transversality conditions $\lambda_i(T) = 0$ for $1 \le i \le 4$.

Setting $\frac{\partial H}{\partial u_i} = 0, i = 1,2$, we obtain $u_1 = \frac{-\lambda_3 s_1}{c_1}$ and $u_2 = \frac{-\lambda_4 s_2}{c_2}$. Since u_1 and u_2 are bounded, $0 \le u_1, u_2 \le 1$, the characterization of the optimal control pair is therefore given by

$$u_1^*(t) = min\{1, max\{0, \frac{-\lambda_3 s_1}{c_1}\}\} \quad (7)$$

$$u_2^*(t) = min\{1, max\{0, \frac{-\lambda_4 s_2}{c_2}\}\}$$

Provided $c_i > 0, i = 1,2$. Above discussion is summarized as follows.

Proposition 3.1. Given an optimal control pair (u_1^*, u_2^*) and solutions of the corresponding state equations (1) there exist adjoint variables $\lambda_i, 1 \le i \le 4$, satisfying

$$\begin{aligned} \lambda_1' &= -1 - \Big(r(1 - 2bx - by) - \frac{\beta gv}{(g+x)^2} - kz\Big)\lambda_1 - \\ &\quad \frac{\beta gv}{(g+x)^2}\lambda_2 - mz\lambda_4 \\ \lambda_2' &= rbx\lambda_1 + (a + cz)\lambda_2 - qa\lambda_3 - \frac{phz}{(h+y)^2}\lambda_4 \\ \lambda_3' &= \frac{\beta x}{g+x}\lambda_1 - \frac{\beta x}{g+x}\lambda_2 + (\delta + \gamma z)\lambda_3 \\ \lambda_4' &= kx\lambda_1 + cy\lambda_2 + \gamma v\lambda_3 - (-d + mx + \frac{py}{h+y})\lambda_4 \end{aligned} \quad (8)$$

$\lambda_i(T) = 0$ for $1 \le i \le 4$.

Moreover, u_1^*, u_2^* are represented by (7)

The optimality system, which includes the state and adjoint system is given by,

$$\begin{aligned} x' &= rx\big(1 - b(x + y)\big) - \frac{\beta xv}{g + x} - kxz \\ y' &= \frac{\beta xv}{g + x} - ay - cyz \\ v' &= qay - \delta v - \gamma vz + s_1 \min\{1, \max\{0, \frac{-\lambda_3 s_1}{c_1}\}\} \\ z' &= s - dz + \frac{b_e xz}{k_e + x} - \frac{d_e xz}{k_d + x} + \\ &\quad \frac{pyz}{h+y} s_2 min\{1, max\{0, \frac{-\lambda_4 s_2}{c_2}\}\} \\ \lambda_1' &= -1 - \Big(r(1 - 2bx - by) - \frac{\beta gv}{(g+x)^2} - kz\Big)\lambda_1 - \\ &\quad \frac{\beta gv}{(g+x)^2}\lambda_2 - mz\lambda_4 \\ \lambda_2' &= rbx\lambda_1 + (a + cz)\lambda_2 - qa\lambda_3 - \frac{phz}{(h+y)^2}\lambda_4 \\ \lambda_3' &= \frac{\beta x}{g+x}\lambda_1 - \frac{\beta x}{g+x}\lambda_2 + (\delta + \gamma z)\lambda_3 \\ \lambda_4' &= kx\lambda_1 + cy\lambda_2 + \gamma v\lambda_3 - (-d + mx + \frac{py}{h+y})\lambda_4 \end{aligned}$$

$x(0) > 0, y(0) \ge 0, x(0) + y(0) < \frac{1}{b}$,
$v(0) \ge 0, z(0) \ge 0 \quad \lambda_i(T) = 0$ for $1 \le i \le 4$.

Optimality system (3) results in a two-point boundary value problem. As demonstrated in [19], the solution of (3) is unique if $T > 0$ is small.

4 Numerical Investigations

To analyze the theoretical discussion using optimal control theory, we employ the backward-forward sweep method, as detailed in [18], in conjunction with the fourth-order Runge-Kutta scheme to solve the optimality system (3) numerically. MATLAB software is used for computations. Our numerical analysis begins with the monotherapy of OVT, and the progresses of the monotherapy of ACT, and concludes with the evaluation of the combined treatment of OVT and ACT.

When applying only OVT, the immune cell supply from outside the body is set to zero, which is represented by setting$c_2 = s_2 = 0$. The fixed parameter values are as follows:

$r = 0.346, b = 1.02 \times 10^{-9}, a = 1.333, c = 1.8$
$q = 100, d = 2, \delta = 1.83, p = 2.4 \times 10^{-4},$
$h = 5 \times 10^4, g = 10^5, s = 5000, b_e = 1,$
$k_e = 500, k_d = 25000$

We vary the parameter values of β, γ, d_e, and k. Unless otherwise specified, $c_1 = 10$and $c_2 = 10$ are used for the corresponding therapies. However, changing these values produces similar simulation results.

Before conducting numerical explorations, we suppose to present a plausible range of parameter values and their sources in Table 1, with baseline values given in Equation (9).

Table 1. Parameter values and sources

parameter	Value	Reference
r	0.2773-0.3466 day^{-1}	estimated
δ	0.024-24 day^{-1}	[12]
γ	0.024-48 cell^{-1}day^{-1}	[12]
p	2.4× 10^{-4} − 2.5day^{-1}	[12]
h	20−5 × 10^4cell	[12]
g	40-10^5cell	[13]
u_1	0-1 dimension less	[18]
u_2	0-1 dimension less	[18]
k	$10^{-5} - 10^{-3}$cell^{-1}day^{-1}	[20]
a	1.333-2.6667 day^{-1}	[20]
c	0.0096-4.8 cell^{-1}day^{-1}	[20]
q	10-1350pfu day^{-1}	[20]
b_e	1 day^{-1}	[20]
d_e	$10^{-3} - 10^3$day^{-1}	[20]
k_e	500cell	[20]
k_d	2.5× 10^4cell	[20]
s	5000 cell day^{-1}	[20]
d	2day^{-1}	[20]
β	6 × 10^{-12} − 0.862 cellpfu^{-1}day^{-1}	[21], [22]
b	1.02 × 10^{-9}cell^{-1}	[23], [24], [25]
s_1	varied pfu day^{-1}	
s_2	varied pfu day^{-1}	

The literature reports a wide range of tumor growth rates. For example, $r\epsilon(0.69,0.97)$ in [22], $r = 0.18$ in [24]. The review paper, [22] includes simulated tumour growth rates 0f 0.23,0.43, and 1.636 to illustrated model outcomes. Based on [25], we estimate the tumour growth rates using the doubling time of approximately 45-60 hours for the BxPC-3 cell line, [26], [27], assuming an initial exponential growth phase. These parameter values were also used in the numerical investigations in [28]. BxPC-3 cells are a type of cell line associated with adenocarcinoma and are commonly used in cancer research. In [28], 5×10^6human BxPC-3 cells, which are associated with pancreatic ductal cancer, were subcutaneously injected into mice. After allowing the tumor to grow to a diameter of 5–7 mm, two different oncolytic viruses were injected at a multiplicity of infection (MOI) of 10^8 pfu into different groups of mice. Therefore, the dosage s_1 of OVT typically varies around 10^8pfu.

Additionally, [28], reports that between 10^5 and 2×10^6 T-cells were infused into the experimental mice. For our numerical examples, we use hypothetical values for s_1 and s_2 that are consistent with the values reported in these experiments.

4.1 Monotherapy of Oncolytic Viruses

We explore the scenario where only OVT is applied by setting $c_2 = s_2 = 0$.

Firstly, we set the strength of OVT to $s_1 = 10$ and the cost coefficient to $c_1 = 10$, with a fixed treatment period of 100 days ($T = 100$) The initial conditions are chosen as $(x(0), y(0), v(0), z(0)) = (2 \times 10^7, 0,0,300)$.

In this subsection, we investigate optimal treatment strategies numerically. Parameter values are set according to those given in (9), with $b_e = 1$. We will divide the discussion to monotherapy of OVT, monotherapy of ACT, and the combined treatment of OVT and ACT in the following subsections. Unless otherwise stated, we use $c_1 = c_2 = 10$. In the following numerical examples, susceptible tumor sizes without therapy are denoted by $x(t)$, while those under optimal therapy are represented by $x^*(t)$, plotted in the top row. The bottom row displays the corresponding optimal controls $u^i(t)$. In Figure 1, we fix$\gamma = 0.15$, $k = 10^{-4}$, $d_e = 10^3$, and the initial condition$(2 \times 10^7, 0,0,300)$. Panels (a) and (b) of Figure 1 correspond to scenarios where $\beta = 0.6$ and $\beta = 0.2$, respectively. Further, s_1 is set to 10^8 for Panel (a) and 10^5 for Panel (b) of Figure 1. Two scenarios demonstrate tumor eradication; however, achieving this goal requires a longer treatment period and smaller dosages, as seen in the comparison between

Panels (a) and (b). When the infection rate β is reduced, as shown in Panels (c) and (d) of Figure 1, tumor eradication remains feasible, though it necessitates a long treatment period, particularly with smaller values of s_1.

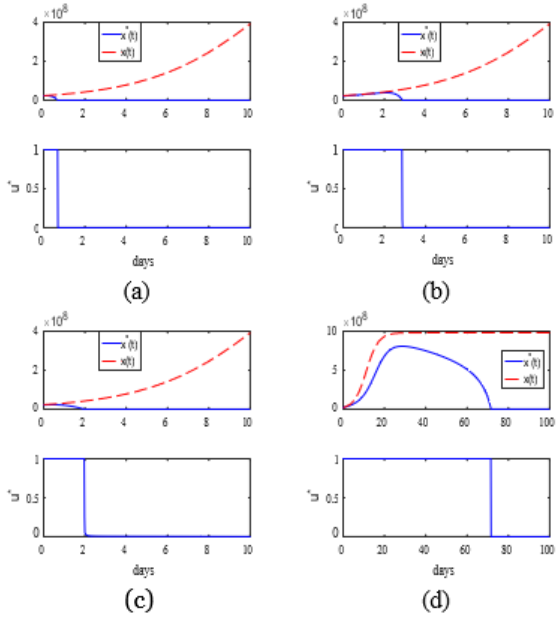

Fig. 1: $\gamma = 0.15$, $k = 10^{-4}$, and $d_e = 10^3$ with initial condition $(2 \times 10^7, 0, 0, 300)$. (a) $\beta = 0.6$, $s_1 = 10^8$. (b) $\beta = 0.6$, $s_1 = 10^5$. (c) $\beta = 0.2$, $s_1 = 10^8$. (d) $\beta = 0.2$, $s_1 = 10^7$. Reducing the dosage requires extending the duration of the therapy. Conversely, decreasing the viral infection rate leads to a longer time needed to reduce the cancer load

In Figure 2, we set $d_e = 10^3$ and $s_1 = 10^8$ while varying the infection rate β and the viral killing rate γ. Tumor elimination by day 15 is observed in panels (b) and (c) when γ is small, whereas in panel (a), tumor control is achievable only if γ is larger. In plot (d), where $k = 10^{-5}$ is smaller, a longer treatment period is required to eradicate the tumor. Similarly, in Figure 2(e), when $k = 10^{-3}$ is large and i $\gamma = 0.25$ s also larger, a prolonged treatment period is necessary. In each plot, the blue curve represents the tumor size with therapy, while the red dashed curve represents the tumor size without therapy. Figure 2 illustrates that as k increases, it becomes easier to reduce the tumor size. Additionally, decreasing the killing rate of viral cells by immune cells enhances the effectiveness of the therapy.

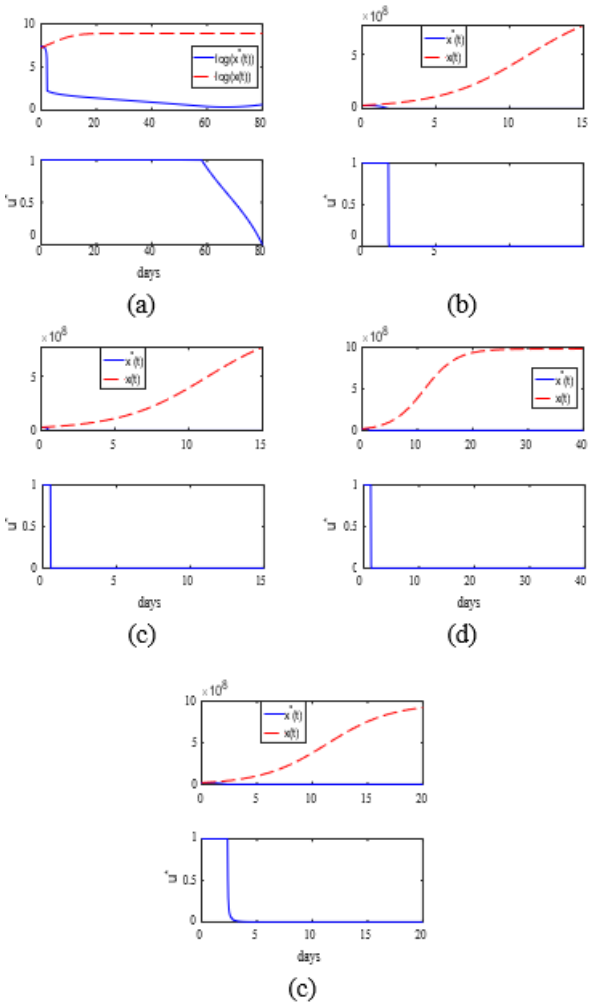

Fig. 2: $d_e = 10^3$ with initial condition$(2 \times 10^7, 0,0,300)$. (a) $k = 10^{-4}$, $\beta = 0.4$, $\gamma = 1.0$ and $s_1 = 10^8$. (b) $k = 10^{-4}, \beta = 0.2, \gamma = 0.09$ and $s_1 = 10^8$ (d) $k = 10^{-5}, \beta = 0.6, \gamma = 0.15$ and $s_1 = 10^7$ (e)) $k = 10^{-3}$, $\beta = 0.2$, $\gamma = 0.25$ and $s_1 = 10^8$

4.2 Monotherapy of Adoptive Cell Transfer

In this subsection, we explore the monotherapy of adoptive cell transfer (ACT), setting $c_1 = s_1 = 10$. As in [8], if there are no viruses and infected tumor cells initially $(v(0) = y(0) = 0)$, it is sufficient to consider the xz-subsystem with ACT, as the parameters β and γ do not influence the simulations. The results are presented in Figure 3.

First, observe that ACT is applied throughout all the treatment period. In Figure 3(a), with a large immune exhaustion rate of $d_e = 10^3$ and an initial tumor size of 2×10^8, the tumor is controlled by the therapy but cannot be eradicated. Reducing d_e to 200, as shown in Figure 3(b), results in a significantly smaller treated tumour compared to Figure 3(a) illustrates that with $d_e = 600$, the tumour can only be controlled but not eradicated. Increasing the tumour-killing rate to $k = 10^{-3}$, as

seen in Figure 3(d), leads to a reduction in tumour size during the treatment period.

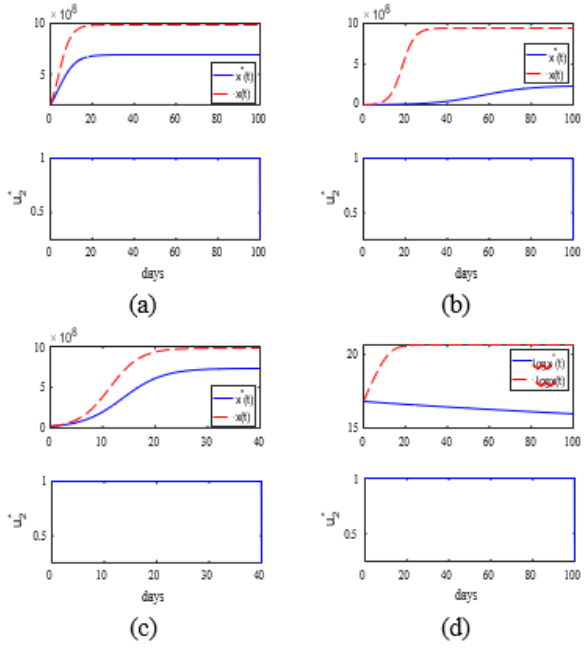

Fig. 3: (a) $k = 5 \times 10^{-4}, d_e = 10^3, s_2 = 2 \times 10^5$with initial condition$(2 \times 10^8, 0,0,300)$. (b) $k = 5 \times 10^{-4}, d_e = 200, s_2 = 10^5$ with initial condition $(2 \times 10^7, 0,0,300)$. (c) $k = 5 \times 10^{-4}, d_e = 600, s_2 = 10^5$ with initial condition $(2 \times 10^7, 0,0,300)$. (d) $k = 10^{-3}, d_e = 300, s_2 = 10^5$ with initial condition $(2 \times 10^7, 0,0,300)$. When we decrease the immune exhaustion rate, it becomes evident that the cancer can be more effectively reduced. Additionally, increasing the tumor-killing rate enhances the reduction of tumor levels; however, continuous administration of the therapy is necessary.

4.3 Combined OVT and ACT

In this subsection, we examine the effects of combined therapy involving both OVT and ACT. Initially, let$k = 10^{-3}, \beta = 0.6, d_e = 300, \gamma = 0.49$, and the initial condition be $(2 \times 10^7, 0,0,300)$.
Figure 4(b) offers a detailed view of (a) in the first half-day. It's evident that, despite the application of OVT from[0,1000], the combined therapy is ineffective in panel (a). In Figure 4(c) and Figure (d), both OVT and ACT are applied throughout the whole treatment period. Here, $s_2 = 9 \times 10^4$, significantly larger than $s_2 = 10^3$used in Figure 4(a)-(b). The combined therapy effectively reduces tumor size. Next, we fix the parameter values$\beta = 0.2, \gamma = 0.7$, and $d_e = 200$, and use strengths $s_1 = 6 \times 10^6$and $s_2 = 10^3$ with the initial condition $(2 \times 10^7, 0,0,300)$.

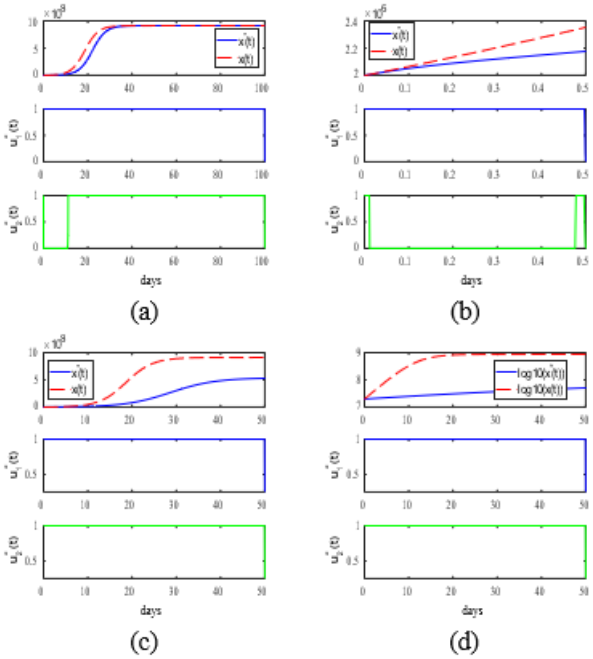

Fig. 4: Parameter values $k = 10^{-3}, \beta = 0.6, d_e = 300, \gamma = 0$ and the initial condition $(2 \times 10^6, 0,0,300)$ are fixed. (a)-(b) $s_1 = 6 \times 10^6$ and $s_2 = 10^3$. (c) $s_1 = 2 \times 10^5$ and $s_2 = 2 \times 10^4$. (d) $s_1 = 2 \times 10^5$ and$s_2 = 9 \times 10^4$. Here, we observe that increasing the dosage makes it easier to reduce the tumor size, but continuous treatment is necessary to achieve this effect.

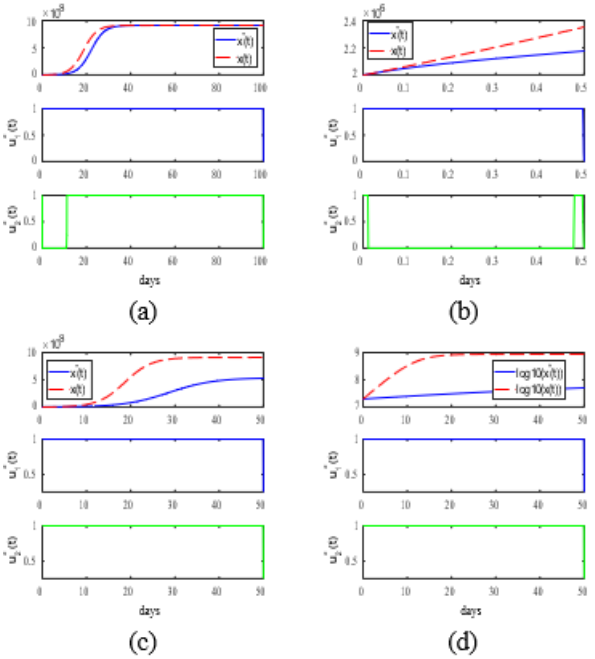

Fig. 5: Parameter values $\beta = 0.2, \gamma = 0.7, d_e = 200, s_1 = 6 \times 10^6, s_2 = 10^3$ and the initial condition $(2 \times 10^7, 0,0,300)$ are fixed. (a) $k = 3 \times 10^{-4}$. (b) $k = 5 \times 10^{-4}$.(c) $k = 6 \times 10^{-4}$.(. (d) $k = 7 \times 10^{-4}$. At this stage, we adjust the killing

rate of tumor cells. It is evident that increasing the killing rate makes it easier to reduce the tumor size, but both therapies need to be administered continuously.

We vary the tumor killing rate k, and the results are displayed in Figure 5. It is clear that increasing the anti-tumor killing rate improves the success of the therapy. However, in both numerical examples Figure 4 and Figure 5, the anti-tumor killing rate γ is relatively high, necessitating the use of both types of therapy all the entire treatment period.

5 Summary and Conclusion

We apply optimal control theory techniques to a model incorporating half-saturation effects in tumor proliferation and exhaustion [29]. We explore the effectiveness of Oncolytic Viral Therapy and Adoptive Cell Transfer both individually and in combination over short time periods. Previously, in [29], optimal control strategies were applied to the base model introduced in [8]. In [9], the model from , was modified to incorporate Michaelis-Menten kinetics, introducing saturation effects for the considering immune cells, [19], [30], [31].

From this research, our objective is to minimize the number of susceptible tumor cells while accounting for the costs or tolerances associated with therapy. Since infected cells do not proliferate, our optimization focus excludes them. Although immune cells can remove viruses from Oncolytic Viral Therapy (OVT), the two therapy types do not synergize. In OVT monotherapy, the killing rate of susceptible tumor cells by immune cells is crucial, as increasing this rate leads to reduced tumor level. Similarly, in combined therapy, a higher killing rate of susceptible tumor cells by immune cells improves treatment success. In the context of Adoptive Cell Transfer monotherapy, the rate of immune exhaustion is crucial; reducing this rate decreases tumor levels, as depicted in Figure 3 (Appendix). For the combined therapy, continuous application of both therapies is necessary to achieve efficient results, as given in Figure 5(Appendix). Increasing the anti-tumor killing rate also contributes to the success of the therapy, as shown in Figure 5(Appendix). Furthermore, increasing the initial tumor level from $(2 \times 10^6, 0,0,300)$ to $(2 \times 10^7, 0,0,300)$. necessitates a lower immune exhaustion rate, as indicated in Figures 4 and 5(Appendix). Comparing OVT and ACT treatments in the Figure 5(d)(Appendix) demonstrates that a strong treatment with s_1 and s_2 and $k = 6 \times 10^{-4}$ can eradicate cancer in nearly 100 days. Unlike in [16], ACT proves more valuable in combined therapy. Increasing s_2 aids in tumor reduction, as observed in the simulations shown in Figure 4(Appendix).

References:

[1] Hongming Zhang, Jibei Chen, Current states and future directions of cancer immunotherapy, *Journal of Cancer*, Volume 9, 10, 1773-1781, 2018.

[2] Dong H, Markovic SN, *The Basics of Cancer Immunotherapy*, Springer 2018.

[3] Marelli G, Howells A, Lemoine NR, Wang Y, Oncolytic viral therapy and the immune system: A double-edged sword against cancer, *Front. Immunol*., 9, 1-9, 2018.

[4] Fukuhara H, Ino Y, Todo T, Oncolytic virus therapy: A new era of cancer treatment at dawn. *Cancer Sci*., 107, 1373-1379, 2016.

[5] Heiko Enderling, Mark A.J. Chaplin, Mathematical Modeling of tumor growth and treatment, *Current Pharmaceutical Design*, 20(30), 1-24, 2013.

[6] Gun S, et al., Targeting immune cells for cancer therapy, *Redox Biol*., doi: 10.1016/j.redox.2019.101174, 2019.

[7] Vinay D et al., Immune evasion in cancer: Mechanistic basis and therapeutic strategies, Semin. *Cancer Biol*., 35, S185-S198, 2015.

[8] G.V.R.K. Vithanage, Hsui-Chuan Wei, Sophia Jang, Bistability in a model of tumor-immune system interactions with an oncolytic viral therapy.*AIMS*, 10.3934/mbe.2022072.

[9] G.V.R.K. Vithanage, Hsui-Chuan Wei, Sophia Jang, The role of tumor activation and inhibition with saturation effects in a mathematical model of tumor and immune system interactions undergoing oncolytic viral therapy, *Math. Method Appl. Sci.,* 46(9), 10787-10813, 2023.

[10] Guiot C, et al., Does tumour growth follow a "*universal law*"? J. Theor. Biol., 225, 147-151, 2003.

[11] Anderson RM, Population biology of infectious diseases: Part I, *Nature*, 280, 361-367, 1979.

[12] Storey KM, Lawler SE, Jackson TL, Modeling oncolytic viral therapy, immune checkpoint inhibition, and the complex dynamics of innate and adaptive immunity in glioblastoma treatment, *Front. Physiol*., 11, 1-18, 2020.

[13] Mahasa KJ, Eladdadi A, de Pillis L, Ouifki R, Oncolytic potency and reduced virus tumorspecificity in oncolytic virotherapy. A

mathematical modelling approach, *PLoS ONE*, 12(9), e0184347, 1-25, 2017.
[14] Wodarz D, Viruses as antitumor weapons, *Cancer Res*. 61, 3501-3507, 2001.
[15] Wu JT, Byrne HM, Kirn DH, Wein LM, Modeling and analysis of a virus that replicates selectively in tumor cells, *Bull. Math*. Biol., 63, 731-768, 2001.
[16] G.V.R.K. Vithanage, Sophia Jang, Optimal immunotherapy of oncolytic viruses and adopted cell transfer in cancer treatment, *WSEAS*, 140-149, 2022.
[17] Fleming, W., Rishel, R., *Deterministic and Stochastic Optimal Control, Springer*, New York, 1975.
[18] Lenhart, L., Workman, JT., *Optimal Control Applied to Biological Models, Chapman &* Hall: New York, 2007.
[19] Burden, T., Ernstberger, J., Fister, K., Optimal control applied to immunotherapy, *Dis. Cont. Dyn. Sys*. Ser. B, 4, 135-146, 2004.
[20] Garcia V, Bonhoeffer S, Fu F, Cancer-induced immunosuppression can enable effectiveness of immunotherapy through bistability generation: A mathematical and computational examination, *J. Theor. Biol.*, 492, 110185, 1-16, 2020.
[21] Jenner AL, Yun CO, Kim PS, A Coster CF, Mathematical modelling of the interaction between cancer cells and an oncolytic virus: Insights into the effects of treatment protocols, *Bull. Math. Biol*., 80, 1615-1629, 2018.
[22] Eftimie R, Eftimie G, Tumour-associated macrophages and oncolytic virotherapies: a mathematical investigation into a complex dynamics, *Lett. Biomath*. 5, 6-35, 2018.
[23] de Pillis L, Radunskaya A, Wiseman C, A validated mathematical model of cell-mediated immune response to tumor growth. *Cancer Res.*, 65(17), 7950-7958, 2005.
[24] Kuznetsov VA, Makalkin IA, Taylor MA, Perelson AS, Nonlinear dynamics of immunogenic tumors: parameter estimation and global bifurcation analysis, *Bull. Math. Biol*., 56(2), 295-321, 1994.
[25] Hu X, Ke G, Jang R-J S, Modeling pancreatic cancer dynamics with immunotherapy, *Bull. Math. Biol.*, 81, 1885-1915, 2019.
[26] Deer EL, et al., Phenotype and genotype of pancreatic cancer cell lines, *Pancreas*, 39(4), 425-435, 2010.
[27] Cerwenka A, Kopitz J, Schirmacher P, Roth W, Gdynia G, HMGB1: The metabolic weapon in the arsenal of NK cells, *Mol. Cell. Oncol*., 3, e1175538, 2016.
[28] Koujima T, Tazawa H, Ieda T et al, Oncolytic virus-mediated targeting of the ERK signaling pathway inhibits invasive propensity in human pancreatic cancer, *Mol, Ther, Oncolytics*, 17, 107-117, 2020.
[29] Fidler IJ, Metastasis: quantitative analysis of distribution and fate of tumor emboli labeled with 125i-5-iodo-2′-deoxyuridine, *J. Natl. Cancer Inst*., 4, 773–782, 1970.
[30] Su Y, Jia C, Chen Y, Optimal Control Model of Tumor Treatment with Oncolytic Virus and MEK Inhibitor, *Biomed Res. Int.,* Volume 2016, Article ID 5621313, 2016.
[31] Malinzi J, et al., Enhancement of chemotherapy using oncolytic virotherapy: Mathematical and optimal control analysis, *Math. Biosci. Eng*., 15, 21435-1463, 2018.

Contribution of individual authors to the creation of a scientific article (ghostwriting policy)

Conceptualization: Sophia Jang, RohanaVithanage;
Formal analysis: Rohana Vithanage, Sophia Jang;
Numerical Simulations: Rohana Vithanage, Sophia Jang;
Writing: Sophia Jang, Rohana Vithanage;

Sources of Funding for Research Presented in a Scientific Article or Scientific Article Itself

No funding was received for conducting this study.

Conflict of Interest

The authors have no conflicts of interest to declare.